Journal of Advanced Ceramics
2019, **8**(1): 90–101
https://doi.org/10.1007/s40145-018-0296-y
ISSN 2226-4108
CN 10-1154/TQ

Research Article

Preparation and arc erosion properties of Ag/Ti_2SnC composites under electric arc discharging

Jianxiang DING[a], Wubian TIAN[a,*], Peigen ZHANG[a], Min ZHANG[a], Jian CHEN[a], Yamei ZHANG[b], Zhengming SUN[a,b,*]

[a]*Jiangsu Key Laboratory of Advanced Metallic Materials*, *School of Materials Science and Engineering*, *Southeast University*, *Nanjing 211189*, *China*
[b]*Jiangsu Key Laboratory of Construction Materials*, *School of Materials Science and Engineering*, *Southeast University*, *Nanjing 211189*, *China*

Received: June 21, 2018; Revised: August 17, 2018; Accepted: September 2, 2018

Abstract: New Ag/Ti_2SnC (Ag/TSC) composites with uniform microstructure were prepared by powder metallurgy. The superior wettability between Ag and Ti_2SnC was confirmed with a contact angle of 14°. Arc erosion properties of Ag/10wt%Ti_2SnC (Ag/10TSC) and Ag/20wt%Ti_2SnC (Ag/20TSC) contacts were investigated under 400 V/100 A/AC-3 and compared with Ag/CdO contact. The Ag/10TSC contact exhibited comparable arc erosion property to Ag/CdO contact. The fine arc erosion resistance was attributed to the good wettability between Ti_2SnC and Ag, the good heat-conducting property of Ag/10TSC, and the slight decomposition of Ti_2SnC that absorbed part of electric arc energy. The excessive Ti_2SnC significantly decreased the thermal conducting property of the Ag/20TSC composite, resulting in the severe heat accumulation that decomposed Ti_2SnC and deteriorated arc erosion property. The oxidation behavior of Ti_2SnC under high electric arc temperature was also studied and then an arc erosion mechanism was proposed to get a comprehensive understanding on the arc erosion property of Ag/TSC composites.

Keywords: MAX phase; metal-ceramic composite; arc erosion properties; microstructures; oxidation

1 Introduction

The electrical contact is a critical component in low-voltage switching devices and widely used in a wide range of fields, such as modern electric apparatuses, motor vehicle, airplanes, and space shuttles. The properties of the contact materials directly determine the reliability and lifetime of the switching devices [1]. With excellent electrical contacting properties, Ag/CdO has been utilized by various industries since the beginning of the last century [2]. However, the toxic Cd vapor produced in use endangers the human health and the natural environment, and considerable efforts have been made to find substitute material for Ag/CdO [3]. Some non-toxic contact materials, e.g., Ag/Ni, Ag/SnO_2, Ag/ZnO [1], Ag/TiB_2 [4], Ag/Al_2O_3, Ag/SiC [5], etc., have been studied and developed. But these substitutes have their own problems unsolved presently, including poor formability, large temperature rise, high contact resistivity, poor anti-welding ability and large

* Corresponding authors.
E-mail: W. Tian, wbtian@seu.edu.cn;
Z. Sun, zmsun@seu.edu.cn

material transfer, etc. The disadvantages of these contacts mentioned above primarily originate from their reinforcing phases. For the sake of environment and human health, it is essential to seek new non-toxic reinforcing phase to replace CdO.

In recent years, MAX phases, with the general formula $M_{n+1}AX_n$ (n = 1, 2, 3; M: early transition metal; A: IIIA or IVA group element; X: C or N), have attracted great attention to material scientists [6]. These layered ternary compounds are regarded as promising and attractive materials in the field of structural, electrical, and thermal application, due to their unusual characteristics combining the properties of ceramics and metals. In particular, the combination of high strength, good thermal and electrical conductivity makes MAX a potential reinforcing phase for Ag-based electrical contact materials. Our preliminary work has demonstrated that Ag/10wt%Ti_3AlC_2 composite owned the comparable arc erosion property to the Ag/CdO material [7]. Ti_2SnC is another member of the MAX phase family, which was first discovered by Jeitschko *et al.* [8]. Ti_2SnC is lightweight (6.1 g/cm^3), relatively soft (~3.5 GPa), elastically stiff (~228 GPa in Young's modulus), easily machinable, and a good heat conductor (43 W/(m·K)). It also exhibits a set of superior properties, including high temperature stability, high damage tolerance, superior corrosion resistance, good oxidation resistance, and high thermal shock resistance [9–11]. The combination of these performances makes Ti_2SnC a promising candidate in functional or structural applications. In particular, it was reported that the Ti_2SnC exhibited the lowest electrical resistivity (~0.22 μΩ·m) in the family of MAX phases. The electrical conductivity of Ag/Ti_2SnC composite should be theoretically better than that of Ag/Ti_3AlC_2 composite. That makes Ti_2SnC more suitable to become the reinforcing phase for Ag-based electrical contact materials. In addition, Ti_2SnC has demonstrated its potential in enhancing metal matrix. It was reported that Cu/Ti_2SnC composites were prepared with conventional powder metallurgy process and exhibited good mechanical and electrical properties [12].

The present work focuses on the preparation and property of the Ag/Ti_2SnC composites. Our purpose is to evaluate the potential of Ti_2SnC as the reinforcing phase in the Ag-based contact materials. The research contents of this work are depicted as follows. First, the arc erosion properties of Ag/Ti_2SnC composite were investigated and compared with the commercial Ag/CdO material. Secondly, the influences of the wettability and Ti_2SnC content on the arc erosion properties of the Ag/Ti_2SnC composite were studied and discussed. Then, the microstructure evolution and oxidation behavior of Ti_2SnC in Ag/Ti_2SnC composite at high electric arc temperature were analyzed. Finally, the arc erosion mechanism of Ag/TSC was proposed.

2 Experiment

2.1 Wettability test

The wettability measurement of Ti_2SnC by molten Ag was performed by using the common sessile drop technique. High-purity Ti_2SnC bulk prepared by spark plasma sintering (SPS) was processed into discs (Φ = 10 mm, 2 mm in thickness). Ag bar (~0.05 g, Φ = 2 mm) was placed on the surface of polished Ti_2SnC discs. The Ag–Ti_2SnC pair was placed inside furnace tube of the high-temperature wetting apparatus (OCA15LHT-SV, DataPhysics, Germany). Then the furnace, in a vacuum pressure of 1×10^{-4} mbar, was heated from room temperature to 1200 ℃ for 15 min at a heating rate of 8 ℃/min. The contact angle (θ) data were obtained from the profile by using the analysis software.

2.2 Contact preparation

Ag/TSC composites were prepared by conventional powder metallurgy process. The raw materials for the composites were Ag powder (99.9% purity, ~10 μm) and Ti_2SnC powder (99.0% purity, ~20 μm). The Ag/10wt%Ti_2SnC (Ag/10TSC) and the Ag/20wt%Ti_2SnC (Ag/20TSC) were thoroughly mixed for 0.5 h with a wet ball milling process. After mixing, powders of the Ag/10TSC and the Ag/20TSC were respectively cold pressed into the discs (Φ = 15 mm) at the pressure of 600 MPa. These specimens, with the protection of flowing Ar gas (99.999% purity), were heated to 850 ℃ at a heating rate of 10 ℃/min in a tube furnace and held for 2 h to obtain the Ag/TSC bulk. The densities of the Ag/10TSC and the Ag/20TSC composites were tested by the Archimedes method. Afterwards, these composites were processed into smaller disks (Φ = 7 mm, 1.4 mm in thickness). By means of spot welding, these discs were finally welded to a Cu base for the following electric arc discharging test. The Ag/

12wt%CdO contact (commercial product) was utilized for reference in the test. The basic properties of these three contacts are shown in Table 1.

2. 3 Test of arc erosion property

The Ag/TSC and the Ag/CdO contacts were well assembled in a general contactor to perform the electric arc discharging test. The operation of test was implemented by using a standard electrical arc discharging test instrument at low voltage electrical testing center of the Shanghai Electrical Apparatus Research Institute Group Co. The experiment was carried out under a condition for acceleration in accordance with the national standard of China (GB14048.4-2010). Table 2 shows the experimental parameters of the electrical arc discharging test.

2. 4 Characterization method

The losses of mass in these contacts before and after the electric arc discharging test were determined by the electronic scale (FA2004, China, 0.1 mg in accuracy). Thermal conductivity of Ag/TSC composites (Φ = 12.7 mm, 10 mm in thickness) was tested with a laser thermal conductivity meter (LFA 467HyperFlash, NETZXCH, Germany). The phase constituents of the as-prepared Ag/TSC composites were identified via X-ray diffraction device (XRD, Bruker-AXS D8, Germany) at the scanning speed of 10 (°)/min, and the phase constituents of the eroded Ag/TSC contacts surface were scanned at a slower speed of 0.5 (°)/min. The macro-morphologies of these contacts after electrical arc discharging test were obtained with the digital camera (EOS D60, Canon, Japan). The microstructures of the Ag/TSC composites before and after electrical arc discharging test were observed by a scanning electron microscope (FEI/Philips Sirion 2000, Netherlands). The chemical compositions of contact surfaces were analyzed with an energy dispersion spectrometer (EDS, AZtes X-MAX 80). The polished cross-sections of these eroded contacts were used for the metallography observation, SEM characterization, and element dispersion analysis.

Table 1 Basic properties of the prepared and commercial contacts

Sample	Density (g/cm^3)	Relative density (%)	Hardness (HV)	Resistivity ($10^{-3}\mu\Omega\cdot m$)
Ag/10wt%Ti_2SnC	9.161	93.0	62	141.9
Ag/20wt%Ti_2SnC	8.512	92.6	76	327.1
Ag/12wt%CdO	8.593	98.2	69	50.2

Table 2 Experimental parameters of the electrical arc discharging test

Item	Parameter
Current mode	100 A, 400 V, inductive load
Coil frequency	50 Hz
Operation frequency	6 times/second
Number of operations	2000
Circuit mode	AC-3
Surrounding atmosphere	Air
Ambient temperature	25 ℃

3 Results and discussion

3. 1 Wettability

Fine wettability is beneficial to the preparation and performance of composites [13]. Particularly in the field of composite contact materials, the wettability of reinforcing phase with Ag matrix directly affects the microstructure and the arc erosion properties [14,15]. Therefore, it is necessary to investigate the wettability between Ti_2SnC and Ag before the preparation of Ag/TSC composites. Figure 1 shows the contact angle variation between Ag and Ti_2SnC with the increasing temperature. The contact angle decreased from 65° to 27° at around 987 ℃, then inclined gradually from 27° to 20° in the 987–1020 ℃ temperature range, and finally became steady at a minimum value of 14° at 1025 ℃. The image of the minimum contact angle is shown in the inset of Fig. 1. This result indicates the good

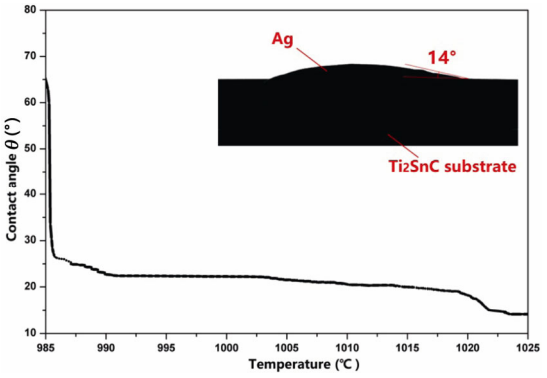

Fig. 1 Contact angle of Ag on Ti_2SnC substrate from 985 to 1025 ℃ and the image of the minimum contact angle (~14°) at 1025 ℃ (the inset).

wettability between Ag and Ti_2SnC. Similar to Ag–Ti_3AlC_2 system [7], the wettability of Ag–Ti_2SnC also belongs to reactive wetting. At high temperatures, Ti–Sn bonds were readily broken and Ti_2SnC was slightly decomposed, and then the interdiffusion between Ag and Sn reduced the interfacial tension of Ag/Ti_2SnC, finally leading to the superior wettability. In addition, the reaction between Ag and Sn enhanced the interface bonding between Ag and Ti_2SnC, which improves its resistance to mechanical damage and arc erosion.

3. 2 Microstructure and phase of the Ag/TSC composites

Figure 2 shows the microstructure and phase constituents of the as-prepared Ag/TSC composites. Both the Ag/10TSC and Ag/20TSC samples exhibited uniform microstructure (Figs. 2(a) and 2(b)). Two major phases, as shown in the enlarged inset of Figs. 2(a) and 2(b), were observed in these samples. The EDS analysis indicated that the light gray phase was Ag and the dark gray phase was Ti_2SnC. Obviously, Ti_2SnC dispersed well in Ag matrix and its amount in Ag/20TSC sample was higher than that of the Ag/10TSC sample. Figure 2(c) shows the XRD patterns of the as-prepared Ag/TSC composites. Besides the main phase of Ag and Ti_2SnC, both composites contained trace amount of C and Sn, which possibly came from the raw material Ti_2SnC powder [16]. The Ag/20TSC composite contained a small amount of Ti–Sn compound (Ti_6Sn_5 and Ti_3Sn), which is due to the slight decomposition of Ti_2SnC.

3. 3 Surface microstructure of eroded contacts

After the electric arc discharging test, the surface morphologies of Ag/10TSC, Ag/20TSC, and Ag/CdO contacts were observed at the optical image, as shown in Figs. 3(a), 3(b), and 3(c), respectively. The Ag/10TSC contact with a clear edge was observed. Half of the Ag/10TSC contact was slightly eroded and the rest was almost unaffected by the electric arc (Fig. 3(a)), which indicates its superior arc erosion resistance. The eroded and unaffected areas were also identified at low- magnification SEM, as shown in Fig. 3(d), where a transition area (the green square) was observed on the contact surface. The Ag/20TSC contact endured severe arc erosion. Its edge was nearly completely damaged by electric arc and its surface was covered by many erosion pits (Fig. 3(b)). Many large holes and cracks were detected on the contact surface (Fig. 3(e)). The Ag/CdO contact presented the slightly eroded edges, where a number of protuberances and dents appeared after arc erosion (Figs. 3(c) and 3(f)).

The microstructural characteristics of the contacts'

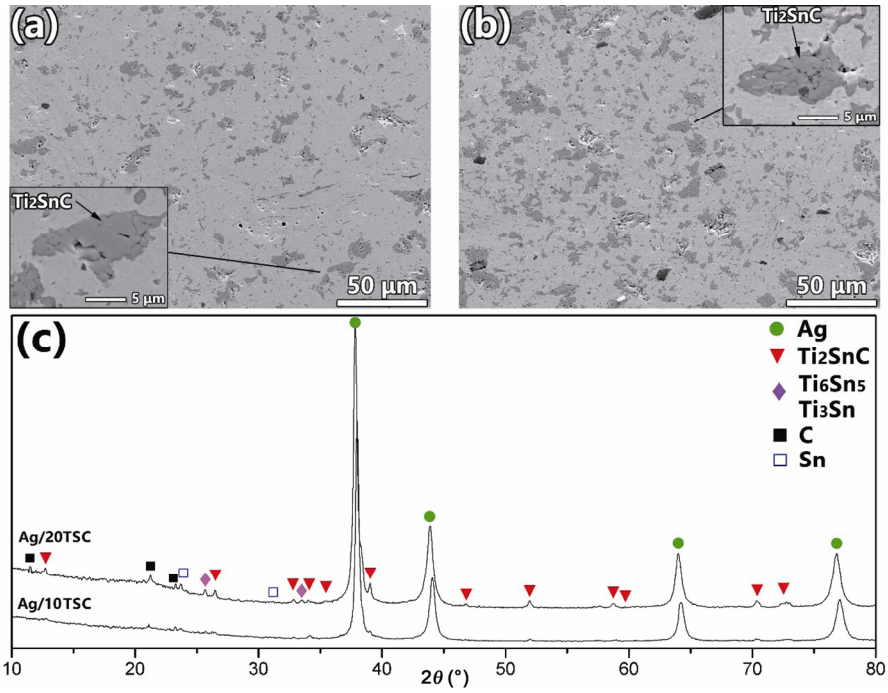

Fig. 2 Microstructures of (a) Ag/10TSC and (b) Ag/20TSC composites. And the insets are the enlarged images of Ti_2SnC. (c) XRD patterns of Ag/10TSC and Ag/20TSC composites.

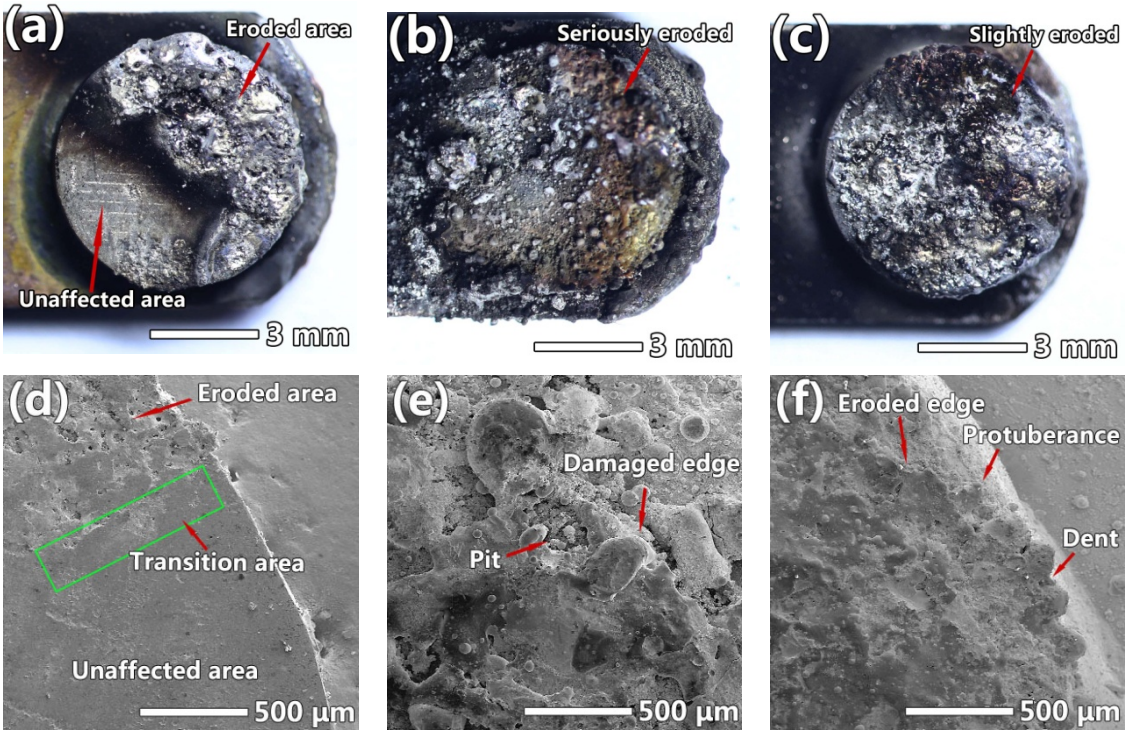

Fig. 3 (a–c) Optical and (d–f) low-magnification SEM images on the surfaces of Ag/10TSC, Ag/20TSC, and Ag/CdO contacts.

surface were further studied at higher-magnification SEM and their chemical compositions were analyzed by EDS. Figure 4(a) shows the typical microstructure of the eroded area on the Ag/10TSC contact surface. The contact surface was mildly eroded by electric arc with the existence of a few small Ag spheres and holes. No traces of macro-cracks were found here. Area 1 was identified to be the Ag molten pool (EDS results not shown), which showed a silk-like surface microstructure (Fig. 4(b)). There were several Ag blocks in molten pool, with visible stripes on its fracture surface (inset in Fig. 4(b)). This was caused by the mechanically electrical arc force and the disconnecting process of the contact spots. There were many shriveled Ag spheres with considerable amount of O element in area 2 (Fig. 4(c)). This was caused by the shrinkage of the liquid Ag and the escape of the oxygen during cooling after the electric arc discharging. A kind of spongy structure was found in area 3 (Fig. 4(d)), which mainly contained Ti and O elements with a little Sn, probably being the decomposed products of Ti_2SnC and the titanium oxides.

Figure 5 shows the characteristic microstructure of the transition area on the Ag/10TSC contact surface. This area was barely affected by the electric arc, where some tiny splashed or deposited Ag particles were observed (inset in Fig. 5(a)), indicating the slight erosion. There were a few erosion pits in this area, with the splashed Ag around them (Fig. 5(b)). In the transition area, Ti_2SnC particles were surrounded by the coarse Ag block (Fig. 5(c)) or the irregularly fine Ag cluster (Fig. 5(d)). Two typical electric arc marks were observed in this area, namely the long tripe-like and meteor crater-like shapes. As shown in Fig. 5(e), the enlarged SEM image shows that the inner of tripe-like structure consisted of many micro arc pits in the size of 0.5–1 μm. This was due to the continuously hitting from the small current column. Figure 5(f) shows the enlarged meteor crater-like pits (with a size of 10–20 μm) that formed when larger current column directly impacted on the contact surface.

Figure 6 shows the representative microstructure of the unaffected region on the Ag/10TSC contact surface. The Ti_2SnC uniformly dispersed in Ag matrix (Fig. 6(a)). The enlarged image exhibited a clear interface between the Ag matrix and the Ti_2SnC particles (Fig. 6(b)) with no trace of holes and cracks, indicating the good bonding between them.

Representative micro-morphologies on the Ag/20TSC contact surface are presented (Fig. 7(a)). There were a plenty of large Ag spheres, big holes, macro-cracks, erosion pits, and molten Ag pools on the contact

surface. The existence of excessive big holes, macrocracks, and pits weakens the strength of Ag matrix, which breaks more easily on the next arcing [14]. This indicated that the Ag/20TSC contact suffered serious arc erosion. Figure 7(b) shows the enlarged image of the Ag molten pool, which exhibits a river-like microstructure. Four typical morphologies of the eroded Ag were detected on the Ag/20TSC contact surface, namely near-spherical, hillock-like, coralloid, and irregular shapes (Figs. 7(c)–7(f)).

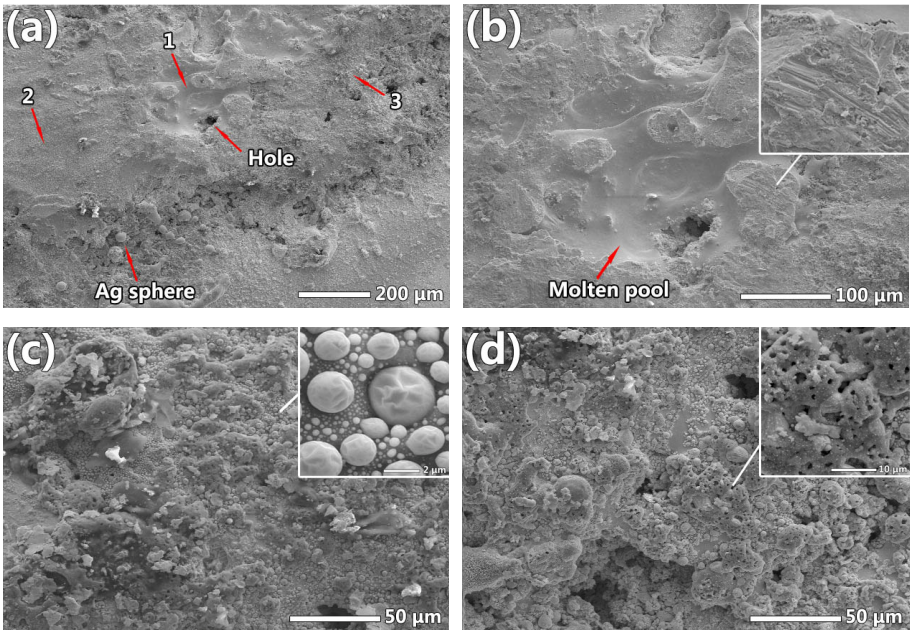

Fig. 4 Representative microstructures of the eroded area on the contact surface of Ag/10TSC. (a) Surface of the Ag/10TSC contact. (b) Amplified image of area 1, and the inset shows the broken Ag with arc marks. (c) Enlarged image of area 2, and the inset shows the sagged Ag particles. (d) Enlarged image of area 3, and the inset shows the spongy Ag.

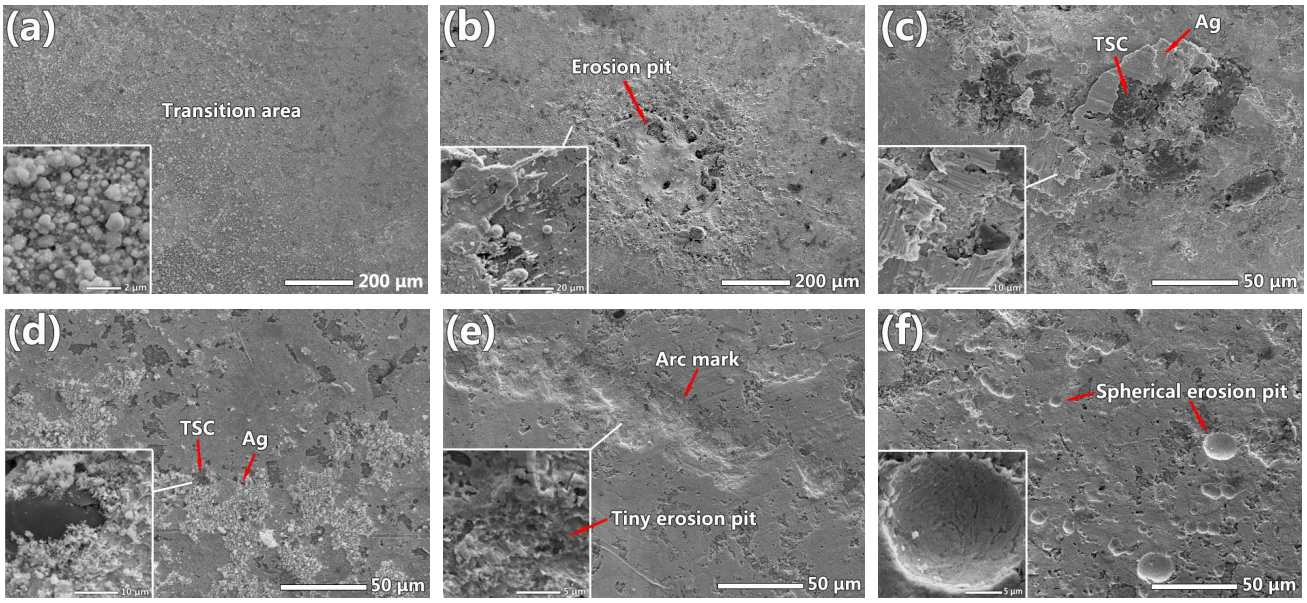

Fig. 5 Primary microstructure of the transition area on the contact surface of Ag/10TSC. (a) Transition area, and the inset shows the magnified image of the irregular Ag particles. (b) Large erosion pit and the arc marks, and the inset shows the magnified image on the edge of the erosion pit. (c) Ti_2SnC particles surrounded by broken Ag blocks, and the inset shows the magnified image of the Ag blocks. (d) Ti_2SnC particles encompassed by tiny Ag cluster, and the inset shows the magnified image of Ag cluster. (e) Arc mark, and the inset shows the magnified image of its inner. (f) Spherical erosion pit, and the inset shows its enlarged inner.

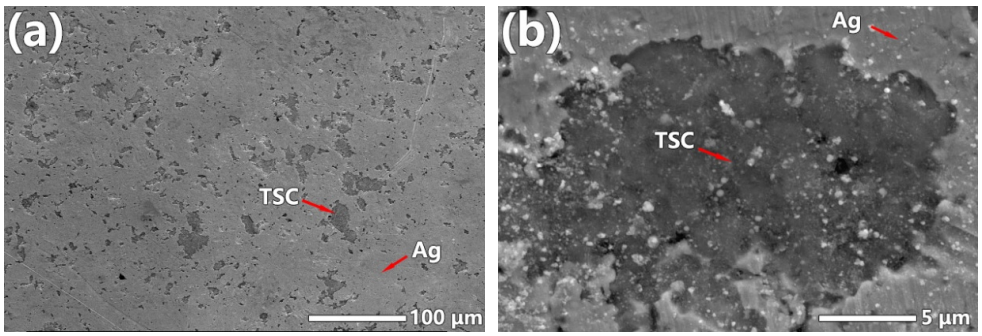

Fig. 6 (a) Representative micro-morphologies of the unaffected region on the contact surface of Ag/10TSC. (b) Enlarged image of Ti_2SnC particle in Ag matrix.

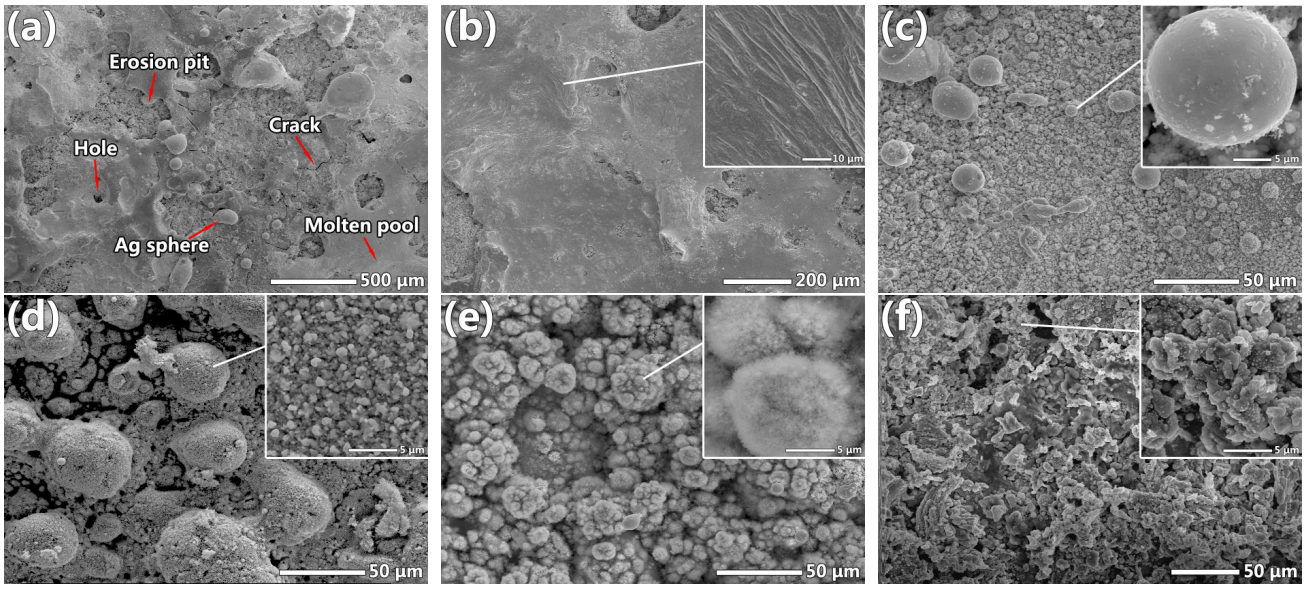

Fig. 7 (a) Typical micro-morphologies on the contact surface of Ag/20TSC. (b) Amplified image of the molten pool, and the inset shows its inner. (c–f) exhibit the different erosion morphologies of the Ag after electric arc discharging, specifically the spherical, the hillock-like, the coralloid, and the irregular. And the insets show their enlarged images.

The representative micro-morphologies on the surface of the eroded Ag/CdO contact after electric arc discharging test are displayed in Fig. 8. The surface morphologies observed in the Ag/20TSC contact, including holes, erosion pits, cracks, molten pools, and Ag spheres, were also found on the surface of the Ag/CdO contact.

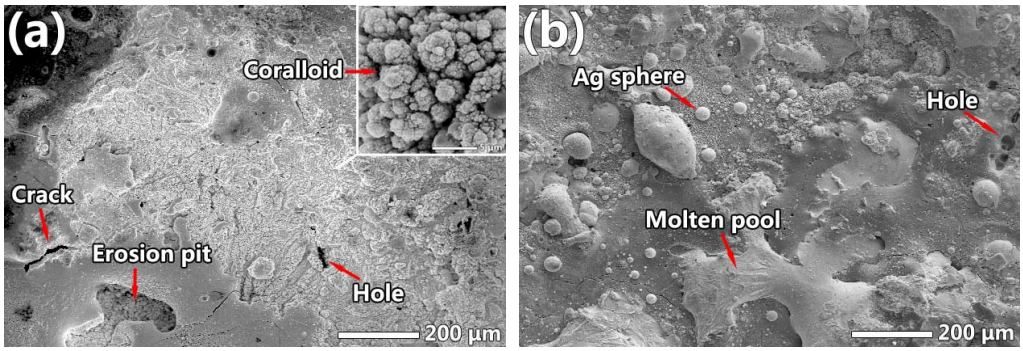

Fig. 8 (a) Primary micro-morphologies on the contact surface of Ag/CdO, where cracks, erosion pits, and holes were clearly observed. (b) Molten pool and the large Ag spheres.

3. 4 Cross section analysis of eroded contacts

The cross sections of the three contacts were observed under optical microscope to further investigate the erosion behavior. The eroded area, the transition area, and the unaffected area were also observed on the cross section of the Ag/10TSC contact (Fig. 9(a)), which is consistent with the aforementioned results of surface observation. Large arc erosion pit was also observed on the cross section of Ag/20TSC contact, which also indicated its poor resistance to material transfer during electric arc discharging (Fig. 9(b)). The contact surface of the Ag/CdO was slightly damaged with the existence of some small erosion pits (Fig. 9(c)).

EDS mapping was utilized to further analyze the cross-sectional element dispersion of the Ag/10TSC and Ag/20TSC contacts. The SEM image (Fig. 10(a1)) shows the top part of the Ag/10TSC contact that consisted of some light grey areas and dark grey areas. Figures 10(a2) and 10(a3) show that the light grey areas were Ag and the dark grey areas were aggregated

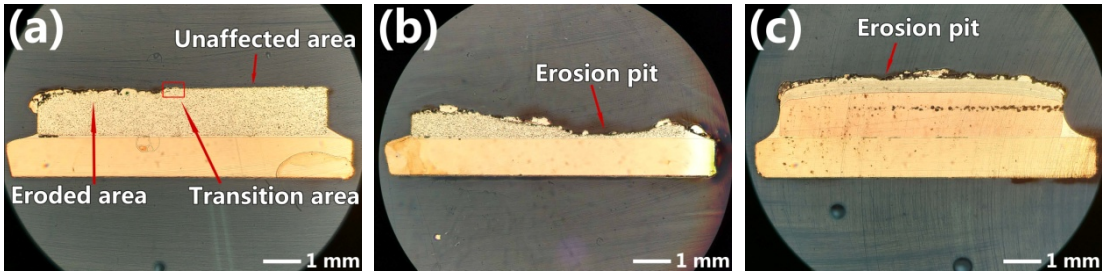

Fig. 9 Cross-sectional OM images of the three contacts after electric arc discharging test: (a) Ag/10TSC, (b) Ag/20TSC, (c) Ag/CdO.

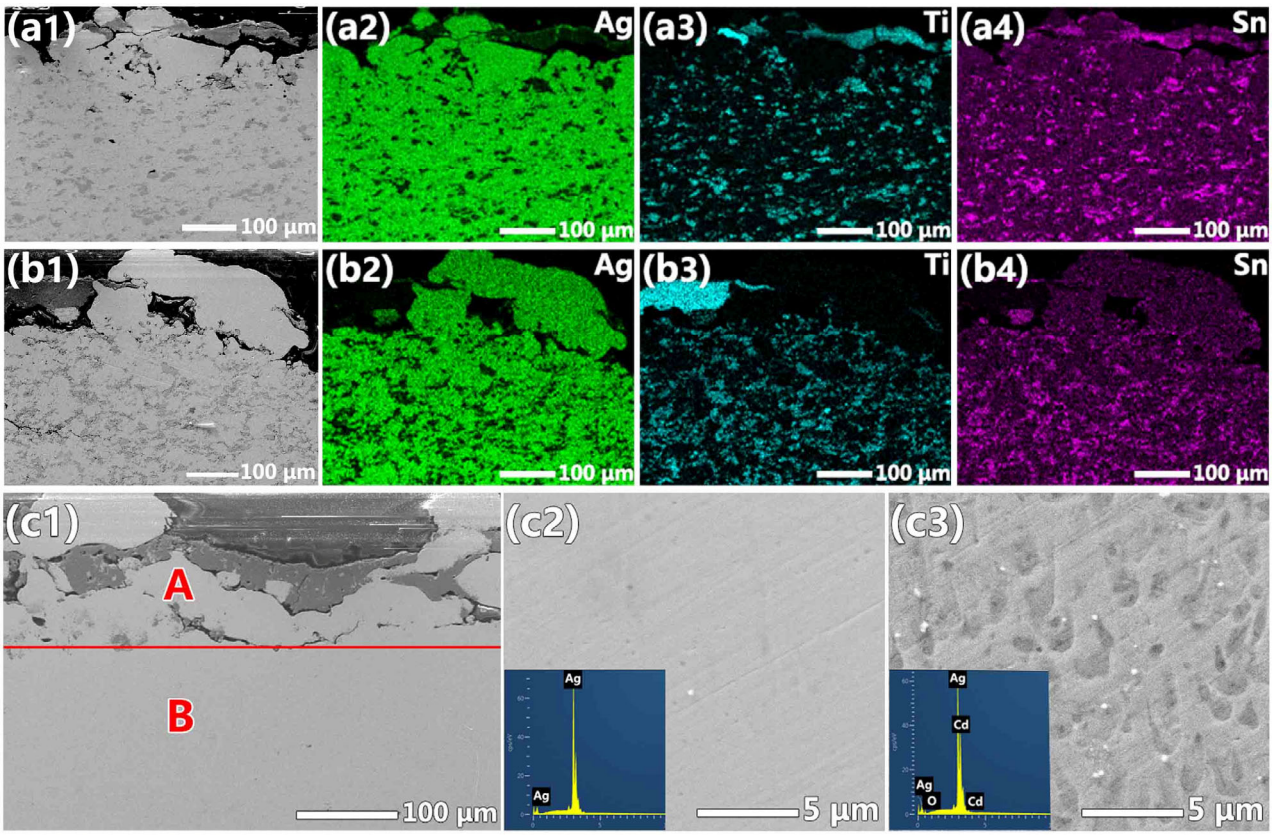

Fig. 10 Cross-sectional element dispersion of the erosion area in different contacts after electric arc discharging. (a1–a4) Ag/10TSC contact. (b1–b4) Ag/20TSC contact. (c1–c3) Ag/CdO contact. (c2) and (c3) show the amplified SEM images and the element composition of the area A and area B in (c1), respectively.

Ti. The distribution of Sn element corresponded well to the position of Ti_2SnC (Fig. 10(a4)). On the top of the cross section in Ag/20TSC contact (Fig. 10(b1)), larger Ag-rich (Fig. 10(b2)) and Ti-rich (Fig. 10(b3)) areas were found. Less Sn were detected on the contact surface as compared with the Ag/10TSC contact (Fig. 10(b4)). The concentration of Ti element and decrease of Sn element on the top part of Ag/20TSC contact indicated the severe decomposition of Ti_2SnC under high electric arc temperature. This further deteriorated its arc erosion resistance. The above results confirmed that the resistances to arc erosion and to material transfer of the Ag/10TSC contact were superior to the Ag/20TSC contact.

Figure 10(c1) exhibits the cross-sectional microstructure and element analysis of the eroded Ag/CdO contact. Two different areas (A and B) were separated by the horizontal line (Fig. 10(c1)). EDS results showed the area A that solely contained Ag element (Fig. 10(c2)), while the area B contained Ag–Cd–O elements (Fig. 10(c3)). This indicated the existence of Ag-rich layer on area A and Ag–CdO on area B. The formation of Ag-rich layer is related to the decomposition of CdO under high electric arc temperature, which has been discussed in our previous work [7].

3. 5 Loss of thickness and mass

The thickness loss results of these three contacts are shown as blue blocks in Fig. 11. The Ag/20TSC contact demonstrated a thickness loss of 88.3%, which is much larger than both the Ag/10TSC contact (11.6%) and the Ag/CdO contact (11.3%). The loss of thickness in these contacts was in accordance with the microstructural results of their surface and cross-section. This further indicated the arc erosion property of Ag/10TSC contact that was superior to the Ag/20TSC contact and comparable to the Ag/CdO contact.

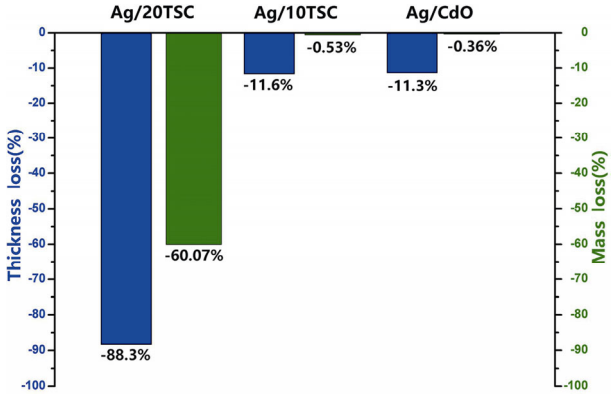

Fig. 11 Loss of thickness (blue blocks) and mass (green blocks) in these contacts after electric arc discharging.

Figure 11 also shows the mass loss results of these contacts (green blocks). The loss of mass in the Ag/20TSC contact (60.07%) was much greater than those of the other two contacts, suggesting its poor resistance to material transfer. However, the Ag/10TSC and Ag/CdO contacts exhibited a slight loss in term of mass (< 1%), which also demonstrated their superior resistance to material transfer.

4 Arc erosion mechanism of the composites

Ag/TSC contact surfaces were further studied with EDS to reveal the arc erosion mechanism of this composite, as shown in Fig. 12. The dark areas (1, 2, 3, 5, 6) and the bright areas (4, 7, 8) were observed on the surface of the Ag/10TSC contact (Fig. 12(a)) and the Ag/20TSC (Fig. 12(b)) contact. And the amount of the dark area in Ag/20TSC is higher than that of Ag/10TSC. The dark areas mainly contained Ti and O with an atom ratio of 1:2, as shown in Fig. 12(c). This indicated the existence of titanium oxides (TiO_x), probably in the form of TiO_2. The bright area mainly consisted of Ag and O, with small amount of Sn. The high content of O element in bright area was due to the rapid dissolution of oxygen in the liquid Ag under high electric arc temperature, and the existence of Sn was attributed to the diffusion of Sn to liquid Ag during electric arc discharging. The increased dark areas on the Ag/20TSC contact surface indicated the severer decomposition of Ti_2SnC and the more Ti_xO_y formed.

In order to further identify the chemical composition of the dark blocks, EDS mapping was used to analyze the element distribution of the Ag/10TSC contact surface (Fig. 13). The distribution shapes of the Ti element (Fig. 13(c)) and the O element (Fig. 13(e)) were consistent with the dark area (Fig. 13(a)), which further demonstrated the existence of Ti_xO_y. The distribution shape of the Ag element (Fig. 13(b)) generally overlapped that of the Sn element (Fig. 13(d)), which confirmed the diffusion of Sn into Ag. The X-ray diffraction was performed on the eroded surface of the Ag/10TSC contact at a slow scanning speed of 0.5 (°)/min to identify the phase constituents. As shown in Fig. 13(g), TiO_2 and Ti_3O_5 were clearly detected besides Ag, which was consistent with the results of EDS analysis.

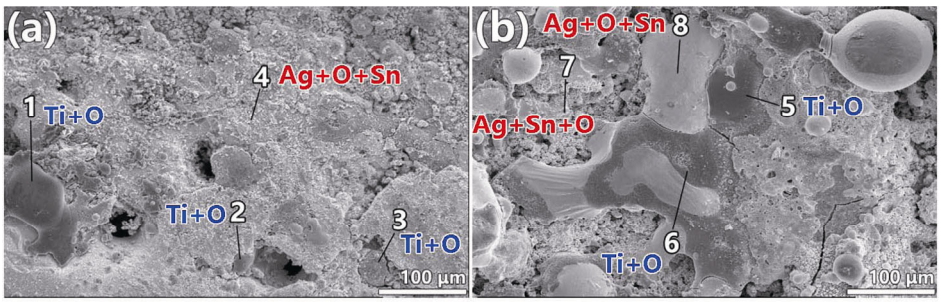

(c)

Cont. / Elem.	Area 1	Area 2	Area 3	Area 4	Area 5	Area 6	Area 7	Area 8
	(at%)	(at%)	(at%)	(at%)	(at%)	(at%)	(at%)	(at%)
C	4.56	4.47	6.35	10.42	4.43	5.41	11.45	
O	64.07	63.24	67.38	49.05	67.84	64.91	18.89	26.37
Ti	31.38	32.29	26.27	2.20	27.73	29.68	1.83	
Ag				34.60			61.60	66.36
Sn				3.72			6.22	7.27
Possible phase	Ti_xO_y	Ti_xO_y	Ti_xO_y		Ti_xO_y	Ti_xO_y		

Fig. 12 Elemental composition on the surface of the Ag/TSC contacts: (a) Ag/10TSC, (b) Ag/20TSC; (c) EDS results of different areas.

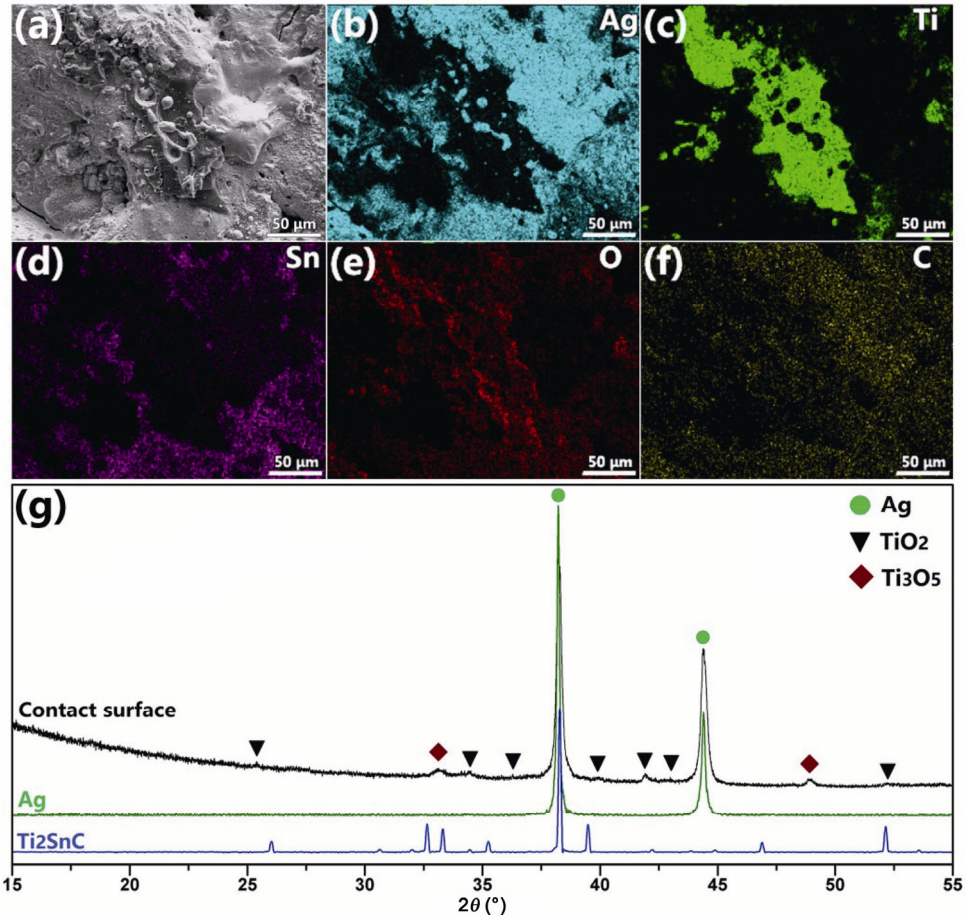

Fig. 13 Element distribution on the surface of the eroded Ag/10TSC contacts after electric arc discharging. (a) SEM image. (b–f) Distribution of the Ag, Ti, Sn, O, C elements in sequence. (g) Phase composition on the surface of the eroded Ag/10TSC contacts after the electric arc discharging.

The arc erosion mechanism of Ag/TSC contacts could be analyzed and understood from the following three aspects. Firstly, the good wettability between Ti_2SnC and Ag matrix significantly affects the arc erosion property of Ag/TSC composites. The Ti_2SnC particles were well wetted by the liquid Ag at high electric arc temperature and uniformly suspended in the liquid Ag molten pool, which increased the molten pool viscosity and the resistance to material transfer. The reactive wetting improved the bonding between Ti_2SnC and molten Ag, and then restricted the flow and the splash of liquid Ag. In other words, the excellent wettability between Ti_2SnC and Ag reduced the erosion loss and finally improved the resistance to arc erosion of Ag/10TSC composite.

Secondly, the arc erosion property of Ag/TSC contacts is related to the thermal effect in the process of the electric arc discharging. The Ag/10TSC composite had high thermal conductivity (a tested value of 78 W/(m·K)). The superior heat-conducting performance contributed to the heat transferring of the Ag/10TSC contact under high electric arc temperature, which decreased its heat accumulation. Only a small amount of Ti_2SnC decomposed during the electric arc discharging process. However, with increasing Ti_2SnC content, the thermal conductivity of the Ag/20TSC composite decreased considerably, to 40 W/(m·K). During electric arc discharging, the low thermal conductivity leads to the apparent heat accumulation of the Ag/20TSC contact and the accelerated damage of Ti_2SnC.

Finally, the high temperature oxidation of Ti_2SnC plays a key role in arc erosion. The electrical arc discharging generated extremely high temperature within several milliseconds [14]. The Ti_2SnC tended to decompose into TiC_x and Sn gradually [9]. Sn was diffused easily into the liquid Ag because of the high solubility of the Sn in the Ag (~13 wt%) [17]. With the increase of ambient temperature, TiC_x was easily oxidized into Ti_xO_y (mainly included TiO_2 and Ti_3O_5) and CO/CO_2, which led to the further decomposition of Ti_2SnC [18]. The lightweight Ti_xO_y floated to the surface layer of the molten pool and formed the aggregation (the dark areas observed under SEM) during cooling. The decomposition of Ti_2SnC would absorb part of electric arc energy, which is beneficial to improving the damage tolerance of Ag/TSC contacts against arc discharging. In some way it has the similar effects to the decomposition of CdO in the use of Ag/CdO [14]. While the excessive loss of Ti_2SnC phase on the Ag/TSC contact surface weakened its restriction ability against the flow and splash of liquid Ag, which introduced more severe damage to the Ag matrix. The competitive action of these factors resulted in the arc erosion property of the Ag/10TSC composite superior to that of the Ag/20TSC composite.

5 Conclusions

An environment-friendly material, Ti_2SnC, was chosen as the reinforcing phase for Ag, and the Ag/Ti_2SnC composites were successfully prepared by pressureless process. The wettability, phase constituent, microstructure, arc erosion properties and mechanism of Ag/10TSC and Ag/20TSC were systematically studied and discussed. The following conclusions can be drawn:

1) The excellent wettability between Ag and Ti_2SnC was confirmed by sessile drop test, and the smallest contact angle reached 14° at 1025 ℃. The reactive wetting process improved the interface bonding of Ag and Ti_2SnC, which benefited arc erosion resistance.

2) Ag/10TSC displayed good surface morphologies and exhibited comparable arc erosion property to the commercial Ag/CdO. That was attributed to the superior wettability between Ti_2SnC and Ag, the good heat-conducting property of Ag/TSC, and the slight decomposition of Ti_2SnC.

3) The surface of Ag/20TSC suffered serious erosion with lots of Ag spheres, molten pools, holes, and cracks. The increased Ti_2SnC content deteriorated the thermal conducting property of the Ag/20TSC, which accelerated the decomposition of Ti_2SnC, resulting in its inferior anti-arc erosion performance.

4) During electric arc discharging, Ti_2SnC was decomposed into TiC_x and Sn gradually. With the increasing temperature, Ti_2SnC was easily oxidized into Ti_xO_y (mainly included TiO_2 and Ti_3O_5). This decomposition process contributed to the absorption of electric arc energy, but the aggregation of Ti_xO_y deteriorated the surface structure and function of Ag/TSC contact.

5) An arc erosion mechanism was depicted to comprehensively understand the different arc erosion behaviors in the Ag/TSC composites.

Acknowledgements

This research was financially supported by the National Natural Science Foundation of China (Grant Nos. 51731004, 51671054, and 51501038), and the Fundamental Research Funds for the Central Universities in China (Grant Nos. 2242018K40108 and 2242018K40109) were highly appreciated.

References

[1] Biyik S, Arslan F, Aydin M. Arc-erosion behavior of boric oxide-reinforced silver-based electrical contact materials produced by mechanical alloying. *J Electron Mater* 2015, **44**: 457–466.

[2] Hao X, Wang X, Zhou S, *et al*. Microstructure and properties of silver matrix composites reinforced with Ag-doped graphene. *Mater Chem Phys* 2018, **215**: 327–331.

[3] Nilsson O, Hauner F, Jeannot D. Replacement of AgCdO by $AgSnO_2$ in DC contactors. In Proceedings of the 50th IEEE Holm Conference on Electrical Contacts and the 22nd International Conference on Electrical Contacts, 2004: 70–74.

[4] Wang X, Li G, Zou J, *et al*. Investigation on preparation, microstructure, and properties of $AgTiB_2$ composite. *J Compos Mater* 2011, **45**: 1285–1293.

[5] Śleziona J, Wieczorek J, Dyzia M. Mechanical properties of silver matrix composites reinforced with ceramic particles. *Journal of Achievements in Materials and Manufacturing Engineering* 2006, **17**: 165–168.

[6] Barsoum MW. The $M_{N+1}AX_N$ phases: A new class of solids: Thermodynamically stable nanolaminates. *Prog Solid State Chem* 2000, **28**: 201–281.

[7] Ding J, Tian WB, Zhang P, *et al*. Arc erosion behavior of Ag/Ti_3AlC_2 electrical contact materials. *J Alloys Compd* 2018, **740**: 669–676.

[8] Jeitschko W, Nowotny H, Benesovsky F. Carbides of formula T_2MC. *J Less-Common Met* 1964, **7**: 133–138.

[9] Barsoum MW, Yaroschuk G, Tyagi S. Fabrication and characterization of M_2SnC (M = Ti, Zr, Hf and Nb). *Scripta Mater* 1997, **37**: 1583–1591.

[10] El-Raghy T, Chakraborty S, Barsoum MW. Synthesis and characterization of Hf_2PbC, Zr_2PbC and M_2SnC (M = Ti, Hf, Nb or Zr). *J Eur Ceram Soc* 2000, **20**: 2619–2625.

[11] Zhou Y, Dong H, Wang X, *et al*. Preparation of Ti_2SnC by solid–liquid reaction synthesis and simultaneous densification method. *Mater Res Innov* 2002, **6**: 219–225.

[12] Wu J, Zhou Y, Yan C. Mechanical and electrical properties of Ti_2SnC dispersion-strengthened copper. *Zeitschrift für Metallkunde* 2005, **96**: 847–852.

[13] Lu JR, Zhou Y, Zheng Y, *et al*. Interface structure and wetting behaviour of Cu/Ti_3SiC_2 system. *Adv Appl Ceram* 2015, **114**: 39–44.

[14] Wang Y, Li H. Improved workability of the nanocomposited $AgSnO_2$ contact material and its microstructure control during the arcing process. *Metall Mater Trans A* 2017, **48**: 609–616.

[15] Wang J, Liu W, Li D, *et al*. The behavior and effect of CuO in Ag/SnO_2 materials. *J Alloys Compd* 2014, **588**: 378–383.

[16] Ding J, Zhang P, Tian WB, *et al.* The effects of Sn content on the microstructure and the formation mechanism of Ti_2SnC powder by pressureless synthesis. *J Alloys Compd* 2017, **695**: 2850–2856.

[17] Karakaya I, Thompson WT, The Ag–Sn (silver–tin) system. *Bulletin of Alloy Phase Diagrams* 1987, **8**: 340–347.

[18] Zhou YC, Dong HY, Wang XH. High-temperature oxidation behavior of a polycrystalline Ti_2SnC ceramic. *Oxid Met* 2004, **61**: 365–377.